A Recessive Mutation in the APP Gene with Dominant-Negative Effect on Amyloidogenesis

Giuseppe Di Fede[1], **Marcella Catania**[1], **Michela Morbin**[1], **Giacomina Rossi**[1], **Silvia Suardi**[1], **Giulia Mazzoleni**[1], **Marco Merlin**[1], **Anna Rita Giovagnoli**[1], **Sara Prioni**[1], **Alessandra Erbetta**[2], **Chiara Falcone**[3], **Marco Gobbi**[4], **Laura Colombo**[4], **Antonio Bastone**[4], **Marten Beeg**[4], **Claudia Manzoni**[4], **Bruna Francescucci**[5], **Alberto Spagnoli**[5], **Laura Cantù**[6], **Elena Del Favero**[6], **Efrat Levy**[7], **Mario Salmona**[4], and **Fabrizio Tagliavini**[1],*

[1]Division of Neurology and Neuropathology, "Carlo Besta" National Neurological Institute, 20133 Milan, Italy.

[2]Division of Neuroradiology, "Carlo Besta" National Neurological Institute, 20133 Milan, Italy.

[3]Division of Neuroepidemiology, "Carlo Besta" National Neurological Institute, 20133 Milan, Italy.

[4]Department of Molecular Biochemistry and Pharmacology, Istituto di Ricerche Farmacologiche "Mario Negri," 20156 Milan, Italy.

[5]Division of Cognitive Disorders, Centro Sant'Ambrogio Fatebenefratelli, Cernusco sul Naviglio, 20063 Milan, Italy.

[6]Department of Medical Chemistry, Biochemistry, and Biotechnology, University of Milan, Segrate, 20090 Milan, Italy.

[7]Departments of Pharmacology and Psychiatry, New York University School of Medicine, and Nathan S. Kline Institute, Orangeburg, NY 10962, USA.

Abstract

β-Amyloid precursor protein (APP) mutations cause familial Alzheimer's disease with nearly complete penetrance. We found an APP mutation [alanine-673→valine-673 (A673V)] that causes disease only in the homozygous state, whereas heterozygous carriers were unaffected, consistent with a recessive Mendelian trait of inheritance. The A673V mutation affected APP processing, resulting in enhanced β-amyloid (Aβ) production and formation of amyloid fibrils in vitro. Co-incubation of mutated and wild-type peptides conferred instability on Aβ aggregates and inhibited amyloidogenesis and neurotoxicity. The highly amyloidogenic effect of the A673V mutation in the homozygous state and its anti-amyloidogenic effect in the heterozygous state account for the autosomal recessive pattern of inheritance and have implications for genetic screening and the potential treatment of Alzheimer's disease.

Acentral pathological feature of Alzheimer's disease (AD) is the accumulation of β-Aβ in the form of oligomers and amyloid fibrils in the brain (1). Aβ is generated by sequential cleavage of the APP by β- and γ-secretases and exists as short and long isoforms, Aβ1-40 and Aβ1-42 (2). Aβ1-42 is especially prone to misfolding and builds up aggregates that are thought to be the primary neurotoxic species involved in AD pathogenesis (2,3). AD is usually sporadic, but

a small fraction of cases is familial (4). The familial forms show an autosomal dominant pattern of inheritance with virtually complete penetrance and are linked to mutations in the APP, presenilin 1, and presenilin 2 genes (5). The APP mutations close to the sites of β- or γ-secretase cleavage flanking the Aβ sequence overproduce total Aβ or only Aβ1-42, respectively, whereas those that alter amino acids within Aβ result in greater propensity to aggregation in vitro (6, 7).

We have identified an APP mutation [Ala^{673}→Val^{673} (A673V)] that causes disease only in the homozygous state. The mutation consists of a C-to-T transition that results in an alanine-to-valine substitution at position 673 (APP770 numbering) corresponding to position 2 of Aβ (Fig. 1A and fig. S1) (8). The genetic defect was found in a patient with early-onset dementia and in his younger sister, who now shows multiple-domain mild cognitive impairment (MCI) (9). Six relatives aged between 21 and 88 years, from both parental lineages, who carry the A673V mutation in the heterozygous state were not affected, as deduced by formal neuropsychological assessment [supporting online material (SOM) text, fig. S2, and table S1], consistent with a recessive Mendelian trait of inheritance. The A673V mutation was not found in 200 healthy individuals and 100 sporadic AD patients. Both mutated and wild-type APP mRNA were expressed in heterozygous carriers (8).

In the patient, the disease presented with behavioral changes and cognitive deficits at the age of 36 years and evolved toward severe dementia with spastic tetraparesis, leading to complete loss of autonomy in about 8 years (SOM text). Serial magnetic resonance imaging showed progressive cortico-subcortical atrophy (fig. S3). Cerebrospinal fluid analysis evidenced decreased Aβ1-42 and increased total and 181T-phosphorylated tau compared with that of nondemented controls and similarly to AD subjects (table S2 and fig. S4) (8). In the plasma of the patient and his A673V homozygous sister, Aβ1-40 and Aβ1-42 were higher than those in nondemented controls, whereas the six A673V heterozygous carriers had intermediate amounts (table S2 and fig. S4).

In conditioned media of fibroblasts prepared from skin biopsies (8), Aβ1-40 and Aβ1-42 were 2.1- and 1.7-fold higher in the patient than in four age-matched controls with no change in Aβ1-42:Aβ1-40 ratio (table S2 and fig. S4), suggesting that the A673V variant alters APP processing, which promotes an increase in Aβ formation. To confirm this, we transiently transfected Chinese hamster ovary (CHO) and COS-7 cells with either mutant or wild-type APP cDNA and measured Aβ in conditioned media by enzyme-linked immunosorbent assay (ELISA) (8). Cells expressing A673V APP had significantly higher amounts of both Aβ1-40 and Aβ1-42 than did cells transfected with wild-type APP, with no change in Aβ1-42:Aβ1-40 ratio (table S2). CHO and COS-7 cells with the A673V mutation also had increased secretion of amino-terminally truncated Aβ species, including Aβ11-40, Aβ11-42, and AβN3pE-42 (table S2). These differences were paralleled by differences in the production of soluble forms of APP (sAPPβ and sAPPα) and of APP carboxy-terminal fragments (C99 and C83) that derived from the amyloidogenic β-secretase or nonamyloidogenic α-secretase processing (8). Fibroblasts of the patient showed increased secretion of sAPPβ and 2.5-fold increase in sAPPβ:sAPPα ratio (mean of three determinations: 0.5) compared with those of four age-matched controls [0.2 ± 0.01 (SD)] as deduced by ELISA. Similarly, the sAPPβ:sAPPα ratio was significantly higher in media from CHO cells expressing the A673V mutation (0.4 ± 0.1) than in media from control cells (0.1 ± 0.03, P =0.03) (Fig. 1B). Immunoblot analysis of cell lysates with an antibody to the carboxy-terminal region of APP (8) showed a 1.9 ± 0.2 increase in C99:C83 ratio in patient's fibroblasts (mean of three determinations: 0.67) compared with that in control fibroblasts (0.35 ± 0.02) and 2.5 ± 0.2 increase in mutated CHO cells (0.52 ± 0.10) compared with that of control cells (0.21 ± 0.05, P = 0.0001) (Fig. 1, C and D).

We then investigated the effects of the A673V mutation on the aggregation and amyloidogenic properties of Aβ by using synthetic peptides homologous to residues 1 to 40 with and without the A-to-V substitution at position 2 (Aβ1-40$_{mut}$ and Aβ1-40$_{wt}$) (8). Laser light scattering measurements over short periods (first 24 hours after sample preparation) showed that the aggregation kinetics was faster for Aβ1-40$_{mut}$ than for Aβ1-40$_{wt}$ and that the time constants of the exponential increase were 1.3 hours and 5.8 hours, respectively (Fig. 2A). Furthermore, although the initial size distribution of particles generated by the two peptides was similar, after 24 hours Aβ1-40$_{mut}$ assemblies were much larger than Aβ1-40$_{wt}$ aggregates (Fig. 2B). Polarized-light and electron microscopy (EM) showed that Aβ1-40$_{mut}$ aggregates with the tinctorial properties of amyloid (i.e., birefringence after Congo red staining) ultrastructurally formed by straight, unbranched, 8-nm-diameter fibrils were already apparent after 4 hours. Amyloid progressively increased up to 5 days, when the samples contained only fibrils organized in dense meshwork (Fig. 3, B, E, H, and K). Aβ1-40$_{wt}$ followed a qualitatively similar assembly path but with much slower kinetics. The 8-nm-diameter amyloid fibrils were first observed after 72 hours, mingled with oligomers and protofibrils (Fig. 3, A and G), and the size and density of congophilic aggregates reached a plateau only after 20 days (Fig. 3, D and J). Similar differences were observed between wild-type and mutated peptides homologous to residues 1 to 42 of Aβ (Fig. 3, M and N), although the aggregation kinetics was faster compared with that of Aβ1-40.

The finding that the A673V mutation strongly boosts Aβ production and fibrillogenesis raises the question of why heterozygous carriers do not develop disease, so we analyzed the effects of the interaction between Aβ1-40$_{mut}$ and Aβ1-40$_{wt}$. Laser light scattering showed that the time constant of aggregate formation of equimolar mixtures of wild-type and mutated peptides was higher (8.3 hours) than the time to aggregate for either Aβ1-40$_{mut}$ (1.3 hours) or Aβ1-40$_{wt}$ alone (5.8 hours) (Fig. 2A) and that the size distribution of particles was lowest both at time 0 and after 24 hours (Fig. 2B). Furthermore, the aggregates formed by peptide mixtures were far more unstable than those generated by either Aβ1-40$_{wt}$ or Aβ1-40$_{mut}$ after dilution with buffer, with a characteristic dissolution time of 8 min. At the same time, no dissolution kinetics was observed for samples of Aβ1-40$_{wt}$ and Aβ1-40$_{mut}$ alone (Fig. 2C). This was confirmed by urea denaturation studies of peptide aggregates (8). Size exclusion chromatography showed that the elution profiles of Aβ1-40$_{wt}$ and Aβ1-40$_{mut}$ were marked by a single peak corresponding to the dimer, whereas the mixture gave a smaller peak area corresponding to the dimer and a second small peak corresponding to the monomer (Fig. 4A). Polarized light and EM showed that the peptide mixture built up much fewer congophilic aggregates than not only Aβ1-40$_{mut}$ but also Aβ1-40$_{wt}$ (Fig. 3, C, F, I, and L). Similar results were observed with Aβ1-42 peptides (Fig. 3, M to O). Amyloid formation was also inhibited when Aβ1-40$_{wt}$ was incubated with a hexapeptide homologous to residues 1 to 6 containing the A-to-V substitution in position 2 (Aβ1-6$_{mut}$) at 1:4 molar ratio (fig. S5).

We analyzed the binding of Aβ peptides with and without the A673V mutation to Aβ1-40$_{wt}$ by using surface plasmon resonance (8). In addition to Aβ1-40$_{wt}$ and Aβ1-40$_{mut}$, we used the hexa-peptides Aβ1-6$_{wt}$ and Aβ1-6$_{mut}$ to evaluate the independent contribution of the amino-terminal sequence containing the mutation. No difference in binding to immobilized Aβ1-40$_{wt}$ fibrils was observed between Aβ1-40$_{wt}$ and Aβ1-40$_{mut}$, consistent with the finding that Aβ aggregation is primarily driven by hydrophobic stretches in the central and carboxy-terminal parts of the peptide (Fig. 4B) (10). However, the amino-terminal fragment Aβ1-6$_{mut}$ showed greater ability to bind to wild-type Aβ1-40 than did Aβ1-6$_{wt}$ (Fig. 4C), indicating that the A-to-V substitution at position 2 favors the interaction between mutant and wild-type Aβ.

Lastly, we treated human neuroblastoma SH-SY5Y cells with Aβ1-42$_{wt}$, Aβ1-42$_{mut}$, or mixtures thereof at 5 μM for 24 hours and assessed cell viability by 3-(4,5-dimethylthiazol-2-

yl)-2,5-diphenyl tetrasodium bromide (8): $A\beta 1-42_{mut}$ was more toxic than $A\beta 1-42_{wt}$, and the mixture was significantly less toxic than either peptide alone (Fig. 4D).

We have identified a mutation in the APP gene showing a recessive Mendelian trait of inheritance. Recently, a homozygous APP mutation (A693Δ) was detected in three AD patients from two Japanese pedigrees (11). Because one out of four heterozygous individuals had MCI, in the absence of experimental studies mimicking the situation in heterozygotes, it is hard to establish whether A693Δ is a recessive mutation or a dominant APP variant with incomplete penetrance.

The A673V APP mutation has two pathogenic effects: it (i) shifts APP processing toward the amyloidogenic pathway and (ii) enhances the aggregation and fibrillogenic properties of Aβ. However, the interaction between mutant and wild-type Aβ, favored by the A-to-V substitution at position 2, interferes with nucleation or nucleation-dependent polymerization, or both, hindering amyloidogenesis and neurotoxicity and thus protecting the heterozygous carriers.

Until recently, the importance of the aminoterminal sequence of Aβ in misfolding and disease was underestimated because this region is highly disordered in the fibrillar form of the peptide (12). However, the amino-terminal domain of Aβ is selectively perturbed in amyloidogenesis, and, most importantly, changes in its primary sequence trigger peptide assembly and fibril formation (13,14). The importance of this domain is further supported by the finding that antibodies against it are optimal for plaque clearance in animal models (15). A previous study reported a distinct heterozygous APP mutation at codon 673 [Ala[673]→Tyr[673] (A673T)] in a participant without clinical signs of dementia (16). Histological analysis did not detect amyloid deposits in the brain. However, when the A673T mutation was introduced in a synthetic Aβ1-40 peptide, it increased the propensity to aggregate, with a much shorter lag phase than that of the wild-type peptide (17). These observations, together with our results, suggest that mutations at position 2 of Aβ confer amyloidogenic properties that lead to AD only in the homozygous state. The finding that the interaction between A673V-mutated and wild-type Aβ hinders amyloidogenesis, and especially the anti-amyloidogenic properties of the mutated six-residue peptide, may offer grounds for the development of therapeutic strategies based on modified Aβ peptides or peptido-mimetic compounds (18,19) for both sporadic and familial AD.

The present data highlight the importance of screening demented and nondemented human populations for mutations of the Aβ encoding region of APP. Genetic variants that could be regarded as normal polymorphisms may turn out to be pathogenic in homozygous individuals. The identification of such mutations would help to prevent the occurrence of the disease in their carriers.

Supplementary Material

Refer to Web version on PubMed Central for supplementary material.

Acknowledgments

References and Notes

1. Hardy J, Selkoe DJ. Science 2002;297:353. [PubMed: 12130773]

2. Selkoe DJ. Physiol. Rev 2001;81:741. [PubMed: 11274343]

3. Walsh DM, et al. Nature 2002;416:535. [PubMed: 11932745]

4. Bertram L, Tanzi RE. J. Clin. Investig 2005;115:1449. [PubMed: 15931380]

5. Rocchi A, Pellegrini S, Siciliano G, Murri L. Brain Res. Bull 2003;61:1. [PubMed: 12788204]

6. George-Hyslop PH. Biol. Psychiatry 2000;47:183. [PubMed: 10682216]

7. Levy E, et al. Science 1990;248:1124. [PubMed: 2111584]

8. Materials and methods are available as supporting material on *Science* Online.

9. Petersen RC, et al. Arch. Neurol 2001;58:1985. [PubMed: 11735772]

10. Cecchini M, Curcio R, Pappalardo M, Melki R, Caflisch A. J. Mol. Biol 2006;357:1306. [PubMed: 16483608]

11. Tomiyama T, et al. Ann. Neurol 2008;63:377. [PubMed: 18300294]

12. Williams AD, et al. J. Mol. Biol 2004;335:833. [PubMed: 14687578]

13. Lim KH. ChemBioChem 2006;7:1662. [PubMed: 17013984]

14. Hori Y, et al. J. Biol. Chem 2007;282:4916. [PubMed: 17170111]

15. Bard F, et al. Proc. Natl. Acad. Sci. U.S.A 2003;100:2023. [PubMed: 12566568]

16. Peacock ML, Warren JT, Roses AD, Fink JK. Neurology 1993;43:1254. [PubMed: 8170579]

17. Meinhardt J, et al. Protein Sci 2007;16:1214. [PubMed: 17525469]

18. Soto C, et al. Nat. Med 1998;4:822. [PubMed: 9662374]

19. Adessi C, et al. J. Biol. Chem 2003;278:13905. [PubMed: 12578830]
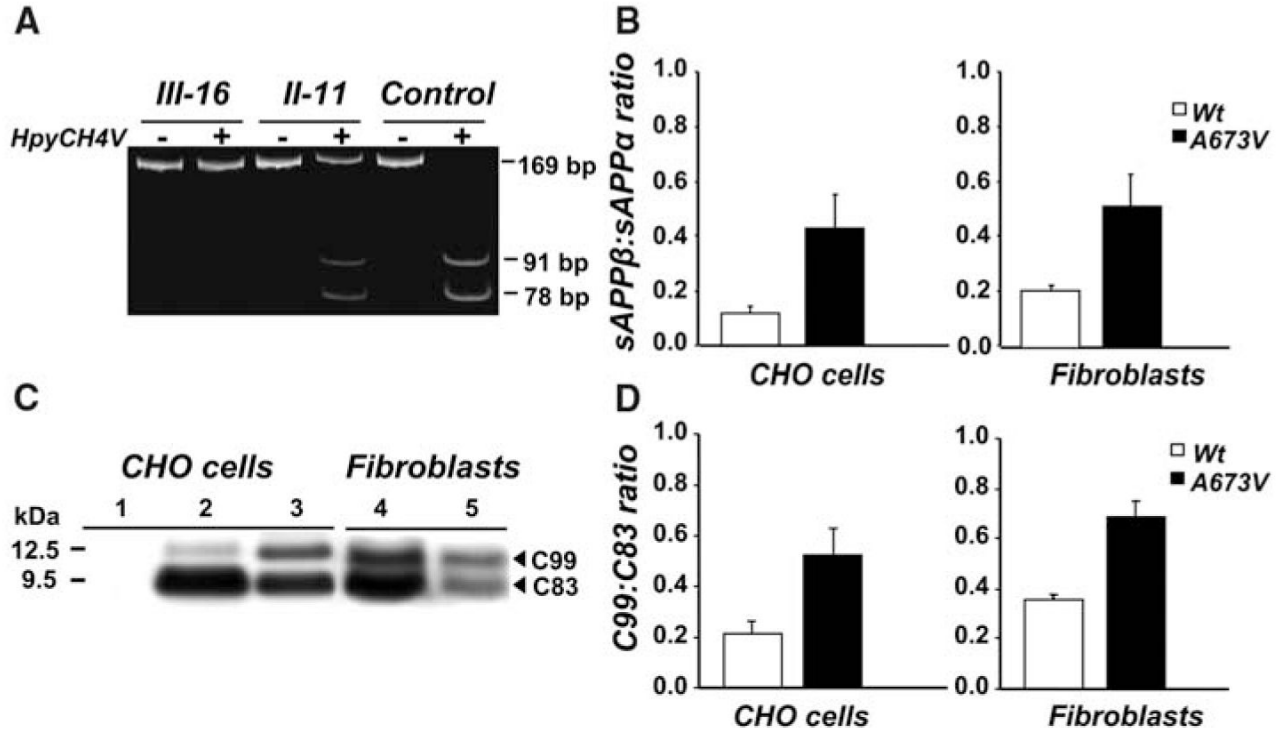
Fig. 1.
Analysis of APP gene and APP processing. (**A**) APP gene analysis by restriction fragment length polymorphism of 169—base pair (bp) polymerase chain reaction (PCR) products amplified from homozygous (III-16), heterozygous (II-11), and control subjects. In the absence of the A673V mutation, the enzyme HpyCH4V generates two fragments of 91 and 78 bp. The mutation abolishes the restriction site, and the PCR product remains uncut. (**B**) sAPPβ:sAPPα ratio in conditioned media from CHO cells transfected with wild-type or A673V-mutated APP and fibroblasts of the proband and four controls. Error bars represent means ± SD. (**C**) APP carboxy-terminal fragments C99 and C83 (arrowheads) in CHO cells transfected with wild-type (lane 2) or A673V-mutated (lane 3) APP and fibroblasts from a control (lane 4) and the proband (lane 5), as shown by immunoblot analysis. Lane 1 corresponds to from nontransfected CHO cells. (**D**) Densitometric analysis of immunoblots, showing a significant increase in the C99:C83 ratio ($P = 0.0001$) in cells carrying the A673V mutation. Error bars represent means ± SD.
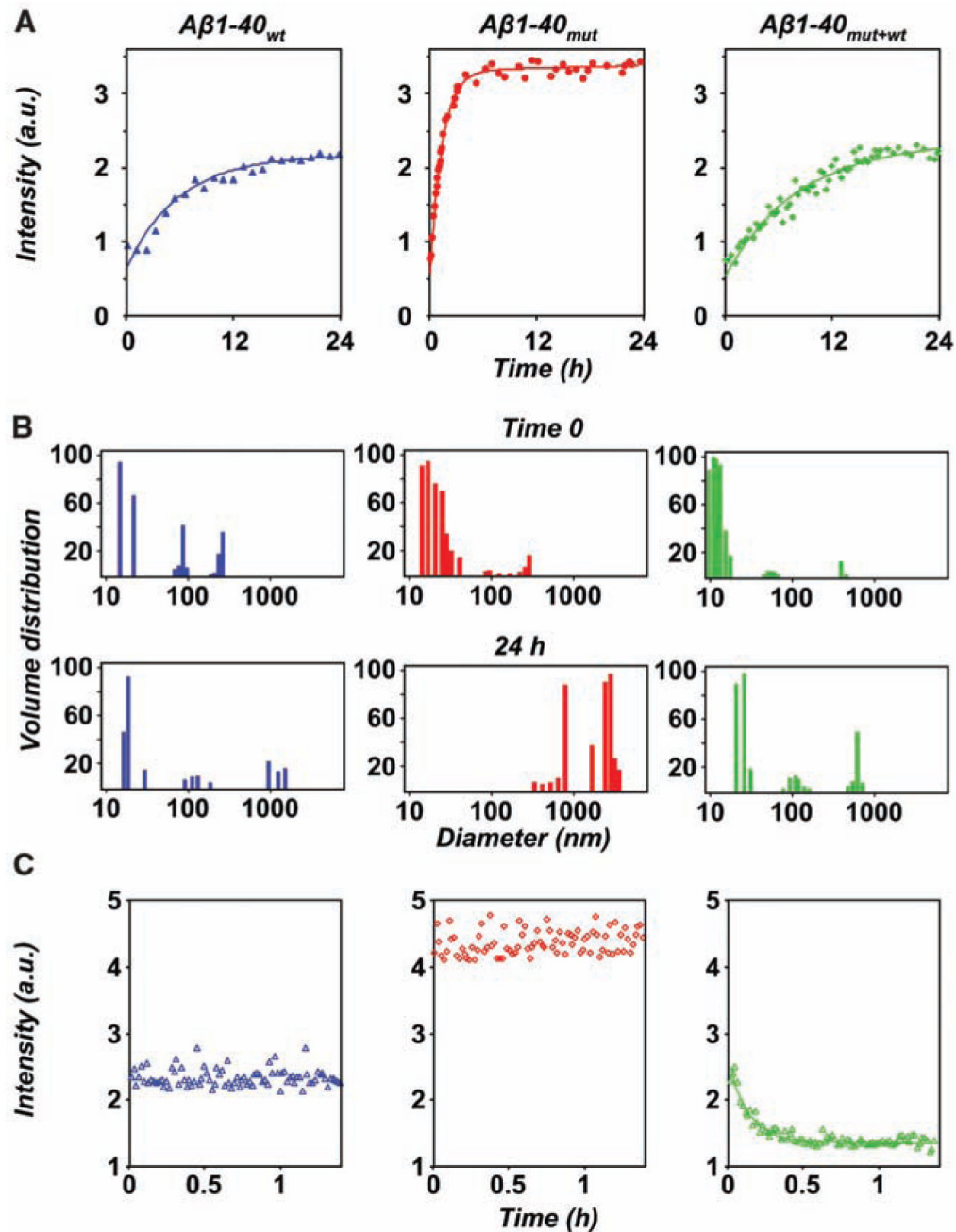
Fig. 2.
Short-time kinetics of Aβ assembly and disassembly, determined by laser light scattering.
(**A**) Course of the light intensity scattered by solutions of Aβ1-40$_{wt}$ (blue), Aβ1-40$_{mut}$ (red),
and their equimolar mixture (green). The corresponding exponential fits are indicated by full
lines. (**B**) Particle size distribution of Aβ1-40$_{wt}$ (blue), Aβ1-40$_{mut}$ (red), and the peptide mixture
(green) immediately after sample preparation (time 0) and after 24 hours. (**C**) Short-time
dissolution kinetics of 48-hour-aged peptide aggregates after fivefold dilution with buffer. a.u.,
arbitrary units.
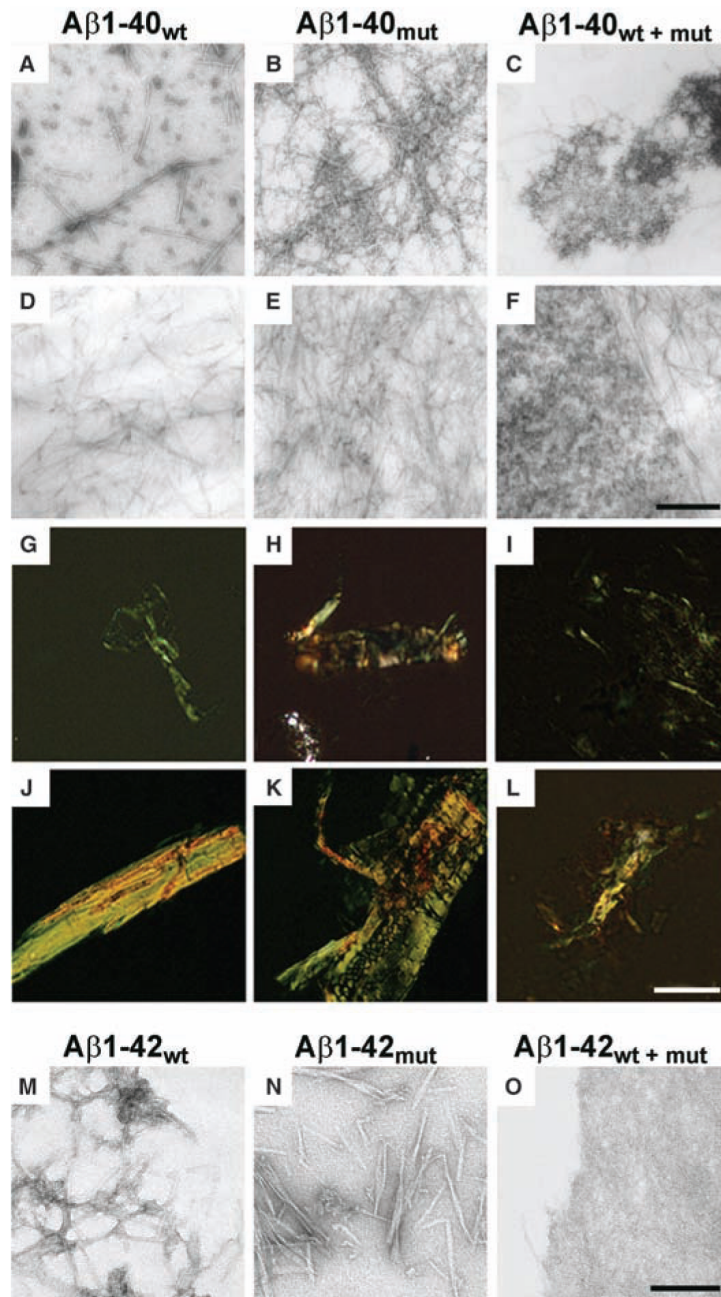
Fig. 3.
Aggregation properties of mutated and wild-type Aβ peptides. (**A** to **F**) Electron micrographs of aggregates generated by Aβ1-40$_{wt}$, Aβ1-40$_{mut}$, and equimolar mixtures after 72 hours [(A) to (C), negative staining] and 20 days incubation [(D) to (F), positive staining]. (**G** to **L**) Polarized light microscopy of Aβ aggregates stained with Congo red after 72 hours [(G) to (I)] and 20 days [(J) to (L)]. (**M** to **O**) Electron micrographs of negatively stained aggregates generated by Aβ1-42$_{wt}$ (M), Aβ1-42$_{mut}$ (N), and equimolar mixtures (O) after 5 days incubation. The peptide mixture contains mainly amorphous material (O), whereas wild-type and mutated Aβ1-42 are assembled in fibrillary structures. Scale bars indicate 250 nm [(A) to (F)], 50 μm [(G) to (L)], and 125 nm [(M) to (O)].
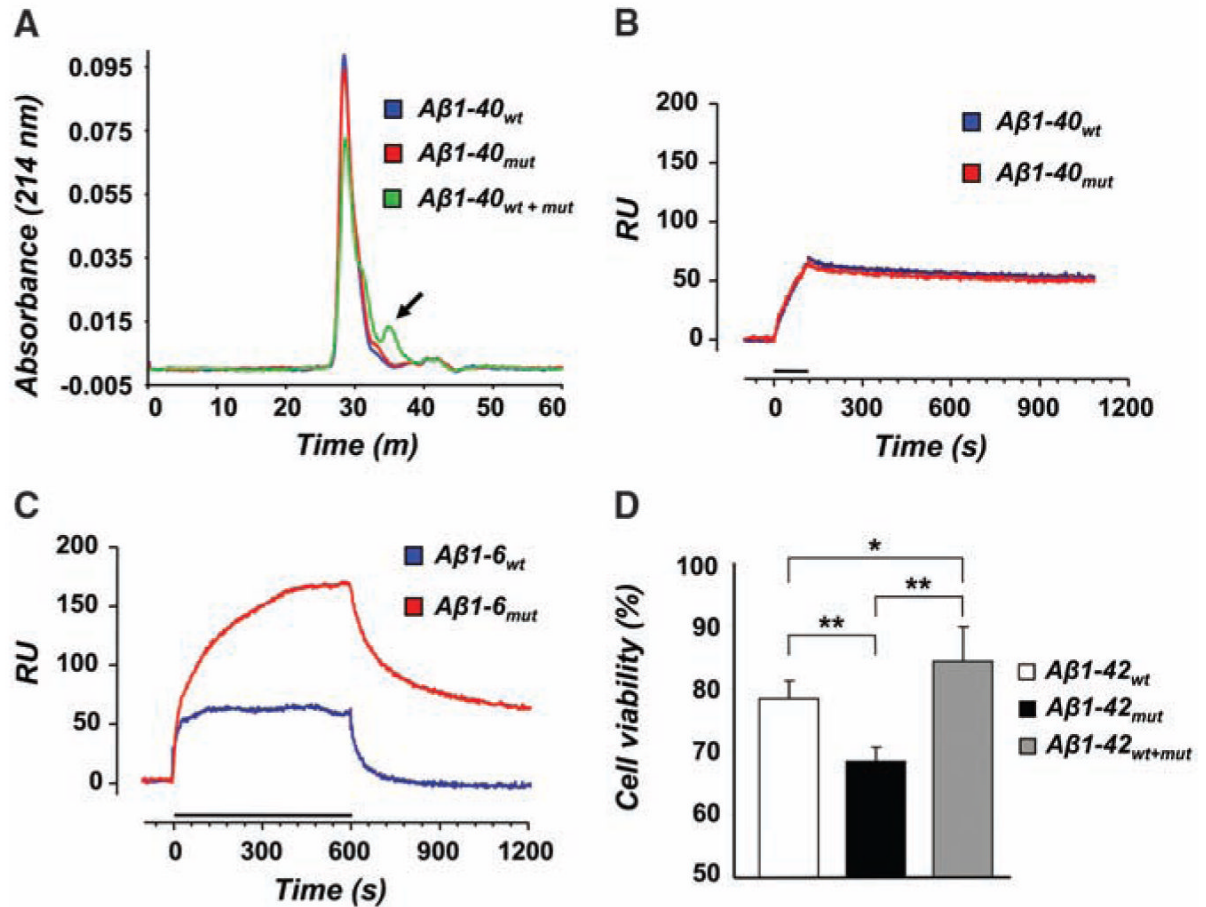
Fig. 4.
Physicochemical and biological properties of mutated and wild-type Aβ peptides. (**A**) Size exclusion chromatograms of Aβ1-40$_{wt}$, Aβ1-40$_{mut}$, and equimolar peptide mixture aggregates after treatment with 1 M urea for 24 hours. Monomeric species (arrow) are only seen in the peptide mixture. (**B** and **C**) Binding of wild-type and mutated Aβ1-40 (B) or Aβ1-6 (C) to amyloid fibrils of Aβ1-40$_{wt}$ determined by surface plasmon resonance. Solutions of Aβ1-40 (1 μM) or Aβ1-6 (500 μM) were injected onto Aβ1-40$_{wt}$ fibrils immobilized on the sensor chip for the time indicated by the bars. (**D**) Viability of human neuroblastoma cells after 24 hours exposure to 5 μM Aβ1-42$_{wt}$, Aβ1-42$_{mut}$, and the equimolar mixture. Error bars represent SD of the mean of eight replicates. *$P = 0.026$, **$P < 0.001$.